Theoretical Temperature-Pressure Phase Diagram for $\{N(CH_3)_4\}_2CuBr_4$

Daniil G. SANNIKOV* and Hiroyuki MASHIYAMA**

Department of Physics, Faculty of Science, Yamaguchi University, Yamaguchi 753-8512

(Received April 24, 2002)

Theoretical phase diagrams for $\{N(CH_3)_4\}_2CuBr_4$ crystal are constructed using the phenomenological approach developed earlier for $\{N(CH_3)_4\}_2MCl_4$ family crystals. Expressions for thermodynamic potentials of the phases presented on the experimental phase diagram, and for boundaries between these phases are derived. The theoretical temperature-pressure phase diagram is plotted and is found to be in agreement with the experimental diagram. The approximations and assumptions made when constructing theoretical diagrams are discussed.

KEYWORDS: phenomenological theory, thermodynamic potential, T-P phase diagram, incommensurate, commensurate, TMATB-Cu compound

§1. Introduction

The crystal $\{N(CH_3)_4\}_2CuBr_4$ (TMATB-Cu) belongs to the large family of well studied tetramethylammonium tetrahalogenometalic compounds $\{N(CH_3)_4\}_2\ MX_4$, where M and X stand for divalent metals and halogens, respectively.[1–3] For many of these crystals the experimental temperature (T) - pressure (P) phase diagram was measured. The theoretical approach to calculation of the T-P phase diagrams for TMATC-M crystals was elaborated in our previous paper.[4] This approach is based on the phenomenological description of a Devil's staircase[5] and on the assumption that the phase diagram contains a special triple point, the Lifshitz-type (LT) point, which was theoretically introduced.[6] The LT-point appeared on the $T-P$ phase diagram due to the assumed existence of two minima of the soft optical branch: one at the center and the other at an arbitrary point of the Brillouin zone.

Note that it is convenient to use the illustrative soft branch concept even when this branch cannot be observed in experiment for one reason or other. The TMATB-Cu crystal differs from the related TMATC-M crystals by the direction of the soft branch wavevector along the b^* axis, instead of the $c*$ axis, in the k-space. However, the approach of ref. 4 is applicable for any (a^*, b^*, c^*) direction. The experimental $T-P$ phase diagram for TMATB-Cu is shown in Fig. 1[7] (see also diagrams for the deuterated compound[8]).

The aim of this paper is to construct theoretical phase diagrams for TMATB-Cu on the bases of the method developed in ref. 4. First we construct the diagram on the plane of dimensionless

* Permanent address: Shubnikov Institute of Crystallography Russian Academy of Sciences, Moscow 117333, Russia.
** E-mail: mashi@yamaguchi-u.ac.jp

coefficients D and A of the thermodynamic potentials (see below). Assuming a linear dependence of D and A on T and P, we then construct the $T-P$ diagram and compare it with the experimental diagram (Fig. 1).

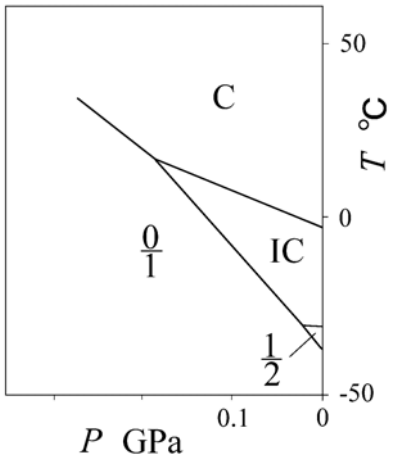

Fig. 1. The experimental $T-P$ phase diagram for TMATB-Cu from ref. 7.

The space group of the initial (C) phase is D_{2h}^{16} or $Pmcn$ (in bca setting, which is usual for these crystals). The modulation vector of the incommensurate (IC) phase is $k_y = qb^*$. The space groups of the commensurate phases $\mathrm{C}_{0/1}$ (with $q=0$) and $\mathrm{C}_{1/2}$ (with $q=1/2$) are ${\mathrm{C}_{2h}}^5$ or $P12_1/c1$ and ${\mathrm{C}_{2v}}^5$ or $Pbc2_1$, respectively.[9)]

Table I, which is an extraction from tables of ref. 10, gives the space groups for all possible $\mathrm{C}_{m/l}$ phases, which correspond to the soft branch. The first column of the table contains the representation of the point group D_{2h} (mmm) according to which the transition from the C phase to the $\mathrm{C}_{0/1}$ phase occurs, then the lowest-rank tensor component which transforms according to this representation, and at last the space group of the $\mathrm{C}_{0/1}$ phase. The next three columns give the space groups of three possible phases c_1, c_2 and c_3 for each $\mathrm{C}_{m/l}$ phase for all $q_{m/l} = m/l$ (m_+, l_+ are even numbers and m_-, l_- are odd numbers) and also the lowest-rank tensor components that have spontaneous values in the c_1 and c_2 phases (for more details, see ref. 10).

Table I. The space groups of all possible commensurate phases corresponding to the soft optical branch with the wavevector $k_y = qb^*$ of the space group $Pmcn$ (D_{2h}^{16}) for TMATB-Cu crystal.

$\frac{0}{1}$				$\frac{m_-}{l_-}$		$\frac{m_+}{l_-}$		$\frac{m_-}{l_+}$	
			c_1	$P112_1/n$	$C_{2h}^5\ (xy)$	$P12_1/c1$	$C_{2h}^5\ (zx)$	$P2_1/b11$	$C_{2h}^5\ (yz)$
$B_{2g}(zx)$	$P12_1/c1$	C_{2h}^5	c_2	$P2_1cn$	$C_{2v}^9\ (x)$	$P2_12_12_1$	$D_2^4\ (xyz)$	$Pbc2_1$	$C_{2v}^5\ (z)$
			c_3	$P11n$	C_s^2	$P12_11$	C_2^2	$Pb11$	C_s^2

§2. Soft branch, thermodynamic potentials and phase boundaries

The soft optical branch or, more exactly, the dependence of the elastic coefficient α on the wave number q is described by the expressions

$$\begin{aligned} \alpha(q) &= \alpha - \delta q^2 - \kappa q^4 + \tau q^6 = a + \Delta(q), \\ \Delta(q) &= \tau(b^2 - q^2)^2[2(b^2 - q_{\rm L}^2) + q^2],\ a = \alpha - \Delta_0, \\ \Delta_0 &= \Delta(0) = 2\tau b^4(b^2 - q_{\rm L}^2),\ \delta = \tau b^2(3b^2 - 4q_{\rm L}^2),\ q_{\rm L}^2 = \kappa/2\tau. \end{aligned} \tag{1}$$

The first expression for $\alpha(q)$ in (1) is more familiar: it represents an expansion of $\alpha(q)$ in powers of q^2, or, better to say, the approximation of $\alpha(q)$ by four-term polinomial, with the last term τq^6 which allows for the branch to have two minima ($\kappa > 0$, $\tau > 0$).[6] The second expression for $\alpha(q)$ in (1) is more convenient introducing two new quantities a and b which are the coordinates of the soft branch minimum at an arbitrary point of the Brillouin zone: $q = b$, $\alpha(b) = a$. The second minimum at the center of the Brillouin zone is determined by the coordinates $q = 0$, $\alpha(0) = \alpha$. The quantity $q_{\rm L}$ specifies the coordinates of the LT point (the LT point is defined by the two minima of the soft branch simultaneously being equal to zero):

$$b = q_{\rm L},\ \Delta(q_{\rm L}) = 0,\ a = 0,\ \Delta_0 = 0,\ \alpha = 0,\ \delta = -\tau q_{\rm L}^4. \tag{2}$$

The two minima exist in the interval of values $-\kappa^2/3\tau < \delta < 0$, or $2q_{\rm L}^2/3 < b^2 < 4q_{\rm L}^2/3$. At $\delta \geq 0$, or $b^2 \geq 4q_{\rm L}^2/3$ the minimum at $q = 0$ becomes maximum, while at $\delta \leq -\kappa^2/3\tau$, or $b^2 \leq 2q_{\rm L}^2/3$ the minimum at $q = b$ disappears. It follows from the latter that the quantities a and b and hence A and D (see below) lose their physical meaning.

We take the expressions of thermodynamic potentials for the C, IC, $C_{0/1}$ and $C_{1/2}$ phases

(which are present on the experimental phase diagram) from ref. 4:

$$\Phi_{\rm C}=0,\ \Phi_{\rm IC}=-a^2/4\beta,\ \Phi_{0/1}=-3\alpha^2/8\beta,$$
$$\Phi_{1/2}=-\alpha_{1/2}^2/4\beta(1-2A_2), \tag{3}$$
$$\alpha_{1/2}=\alpha(q_{1/2}),\ A_2=\mid\alpha_2'\mid/2\beta,\ \Delta_{1/2}=\Delta(q_{1/2}).$$

Note that the expression for $\Phi_{1/2}$ in (3) is valid if the inequality 1-$2A_2>0$, or $\mid\alpha_2'\mid<\beta$ is fulfilled.

Even though the coefficients α, δ, κ, τ and quantities a, b, $q_{\rm L}$ are dimensionless, it is convenient, with the aim of making the expressions more concise, to use in what follows the quantities, which are also dimensionless:

$$A=-\frac{a}{\tau}\frac{1}{Q^6},\ D=\frac{\delta}{\tau}\frac{1}{Q^4},$$
$$B=b\frac{1}{Q},\ Q_{\rm L}=q_{\rm L}\frac{1}{Q},\ Q_{1/2}=q_{1/2}\frac{1}{Q}, \tag{4}$$
$$D_0=\frac{\Delta_0}{\tau}\frac{1}{Q^6}=2B^4(B^2-Q_{\rm L}^2),$$
$$D_{1/2}=\frac{\Delta_{1/2}}{\tau}\frac{1}{Q^6}=(B^2-Q_{1/2}^2)^2[2(B^2-Q_{\rm L}^2)+Q_{1/2}^2].$$

Here Q is merely a number and we take it $Q=0.5$.

By equating potentials (3) to each other we obtain the following expressions for the boundaries between corresponding phases:

$$A=0,\quad A=D_0 \tag{5}$$

for the C-IC and C-$C_{0/1}$ boundaries, respectively.

$$A=c_0D_0,\quad A=c_2D_{1/2},\quad c_0=3+\sqrt{6},\quad c_2=\frac{1}{2A_2}[1+(1-2A_2)^{1/2}] \tag{6}$$

for the IC-$C_{0/1}$ and IC-$C_{1/2}$ boundaries, respectively.

$$A=\frac{1}{c_2-c_0}[c_0(c_2-1)D_0-c_2(c_0-1)D_{1/2}] \tag{7}$$

for the $C_{0/1}$-$C_{1/2}$ boundary. As it follows from eq. (2) the coordinates of the LT point in the variables of eq. (4) are

$$B=Q_{\rm L},\quad A=0,\quad D=-Q_{\rm L}^4. \tag{8}$$

We construct the phase diagram on the $D-A$ plane, since these variables, D and A, are small and therefore their dependences on T and P are essential. The quantity D is expressed according to eqs.(2) and (4) as

$$D=B^2(3B^2-4Q_{\rm L}^2). \tag{9}$$

Setting the values of B^2 we determine the values of A from eqs. (5)-(7) and the values of D from eq. (9), and can construct the $D-A$ phase diagram.

§3. Theoretical phase diagrams

In order to construct the $D-A$ phase diagram for TMATB-Cu crystal, it is necessary to choose the values of $Q_{\rm L}$, and A_2 for the $C_{1/2}$ phase. The choice is based on the best agreement between the theoretical $T-P$ phase diagram, obtained from the $D-A$ diagram, and the experimental phase diagram (Fig. 1). The values are chosen as follows:

$$Q_{\rm L}^2 = 0.8, \quad A_2 = 0.2, \quad Q = 0.5. \tag{10}$$

Figure 2 shows the $D-A$ phase diagram constructed according to expressions (5)-(10). The LT point with coordinates (8) is designated by the letters LT. The $T-P$ phase diagram is constructed from the $D-A$ diagram (Fig. 2) by assuming the simplest linear dependences of D and A on T and P. Then, the T and P axes in Fig. 2 are straight lines. Their position, orientation, and scale are determined from the best agreement with the experimental $T-P$ diagram (Fig. 1). We put $\cot(\widehat{TD}) = \cot(\widehat{PA})$=0.6. Note that the inclination of the T axis to the D and A axes could be determined more precisely if the variation of $q_{\rm inc}$ with T in the IC phase would be known.

Figure 3 shows the theoretical $T-P$ phase diagram constructed on the basis of Fig. 2 with the T and P axes indicated there. From comparison Fig. 3 and Fig. 1 one can see that they are in reasonable agreement.

In summary we list the approximations and assumptions made in the construction of the theoretical $D-A$ and $T-P$ phase diagrams especially as some of them were not mentioned in the text. The triple point between C, $C_{0/1}$ and IC phases existing on the experimental $T-P$ diagram for TMATB-Cu crystal is assumed to be the LT point which was introduced in ref. 6. The single harmonic approximation is used for the IC phase. Only two small quantities D and A are supposed to be dependent on T and P with linear dependence. The remaining quantities $Q_{\rm L}$ and A_2 are considered to be constant, independent of T and P. When constructing the phase diagrams the numerical values of the parameters are taken with a precision of only one significant figure.

We can conclude that the considered here and in ref. 4 phenomenological approach for constructing theoretical phase diagrams are adequate to the experimental phase diagrams.

Acknowledgements

This work was carried out under the Research Program for Special Promotion of the Venture Business Laboratory, Yamaguchi University. One of the authors (D.G.S.) thanks the hospitality while staying the university. He also gratefully acknowledges the financial support of the Russian Fund of Fundamental Research (Grant N 02-00-17746).

---

1) J. D. Axe, M. Iizumi and G. Shirane: *Incommensurate Phases in Dielectrics 2*, ed. R. Blinc and A. P. Levanyuk (North-Holland, 1986, Amsterdam) Chap. 10.

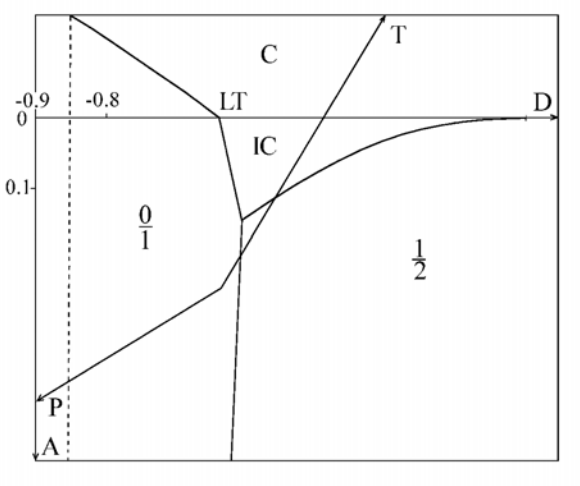

Fig. 2. The $D-A$ phase diagram with the LT point plotted for TMATB-Cu.

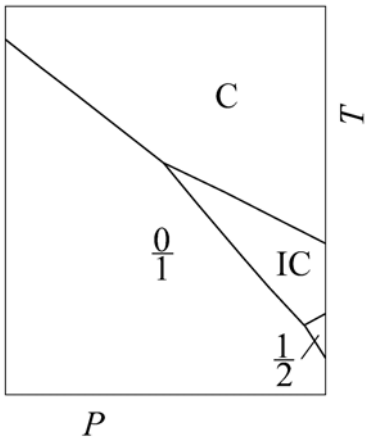

Fig. 3. The theoretical $T - P$ phase diagram plotted on the basis of Fig. 2 for TMATB-Cu.

2) K. Gesi: Ferroelectrics **66** (1986) 269.
3) H. Z. Cummins: Phys. Reports **185** (1990) 211.
4) D. G. Sannikov, G. A. Kessenikh and H. Mashiyama: J. Phys. Soc. Jpn. **69** (2000) 130.
5) D. G. Sannikov: Zh. Eksp. Teor. Fiz. **96** (1989) 2198 [Sov. Phys. JETP **69** (1989) 1244].
6) T. A. Aslanyan and A. P. Levanyuk: Fiz. Tverd. Tela **20** (1978) 804 [Sov. Phys. Solid State **20** (1978) 466].
7) K. Gesi and K. Ozawa: J. Phys. Soc. Jpn. **51** (1982) 2205.
8) K. Gesi: J. Phys. Soc. Jpn. **52** (1983) 2534.
9) K. Hasebe, H. Mashiyama, S. Tanisaki and K. Gesi: J. Phys. Soc. Jpn. **51** (1982) 1045.
10) D. G. Sannikov: Krystallogr. **36** (1991) 813 [Sov. Phys. Crystallogr. **36** (1991) 455].